Electron-hole liquid in germanium under high ⟨111⟩ stress

A. H. Simon,* F. M. Steranka,† and J. P. Wolfe‡
Department of Physics, University of Illinois at Urbana-Champaign, 1110 West Green Street, Urbana, Illinois 61801
and Materials Research Laboratory, University of Illinois at Urbana-Champaign, 104 South Goodwin Avenue, Urbana, Illinois 61801
(Received 14 December 1988)

The properties of the electron-hole liquid (EHL) in Ge are examined as a function of uniaxial ⟨111⟩ stress with use of spectral and temporal measurements of the electron-hole–recombination luminescence. We are the first to observe the EHL phase in the high-stress limit ($\sigma \gtrsim 70$ kgf/mm^2, where 1 kgf/mm$^2 \equiv 10$ MPa) at $T=2$ K, based on fits to calculated spectral line shapes. The dependence of the measured EHL densities on uniaxial ⟨111⟩ stress agrees well with that predicted by sophisticated many-body calculations. Measurements of the EHL lifetime are also reported for uniaxial ⟨111⟩ stresses from 5.6 to 23.9 kgf/mm^2. The density dependence of the EHL lifetime indicates a constant value for the electron-hole enhancement factor, $g_{eh}(0)$, for electron-hole–pair densities $> 3.5\times10^{16}$ cm^{-3}. This result disagrees with theoretical predictions, but is consistent with experimental results reported by others.

I. INTRODUCTION

The existence and properties of an electron-hole liquid (EHL) in a particular semiconductor is critically dependent on the semiconductor's band structure.[1] Generally, indirect-band-gap semiconductors, such as Ge or Si, are favorable for EHL condensation due to their degenerate multivalley band structures. Interesting changes in EHL properties can be brought about by modifying the band structure in a particular material. One technique for altering a semiconductor's band structure is the application of uniaxial stress to the crystal. In this paper, we report on measurements of the EHL density and lifetime in Ge as a function of uniaxial stress. Comparisons will be made to the predictions of many-body theories.[2–8]

Excitons in Ge form as a result of the Coulomb attraction between an electron and a hole. The exciton has a characteristic binding energy ϕ_x and Bohr radius a_x. At temperatures below a characteristic critical temperature T_c, excitons undergo a phase transition into the electron-hole liquid (EHL). At $T=0$ K, the energy $E(n)$ of an electron-hole pair in the EHL is a function of the electron-hole–pair density n and is given by the following expression:

$$E(n)=E_k(n)+E_x(n)+E_c(n)\ , \tag{1}$$

where $E(n)$ is the kinetic energy, $E_x(n)$ is the exchange energy, and $E_c(n)$ is the correlation energy per pair. The ground state of the EHL is characterized by a ground-state density n_0 and energy E_G.

The properties of the EHL have been the subject of much theoretical interest.[1–8] This interest arises because the EHL is an excellent physical example of a many-body system of fermions interacting via a Coulomb potential. The quantitative question critical to the formation of the EHL centers on whether the ground-state energy of the EHL is lower than the exciton binding energy. If $E_G < -\phi_x$, the EHL is the ground state of the electron-hole system and will have a positive binding energy $\phi_l = |E_G| - \phi_x$. If $E_G > -\phi_x$, the EHL will be unstable with respect to the formation of excitons.

The stability of the EHL depends on the band structure, which may be modified by applying stress to the crystal. Stress produces qualitative and quantitative changes at the conduction- and valence-band extrema. A schematic diagram of the Ge band structure as a function of uniaxial ⟨111⟩ stress is shown in Fig. 1. The diagrams are labeled Ge(n_e;n_h), where n_e denotes the number of occupied electron bands and n_h the number of occupied hole bands. Shaded regions in Fig. 1 indicate occupied electronic states in the EHL. In an uncompressed Ge crystal, the ⟨111⟩ conduction-band minima are fourfold degenerate. There are also one light- and one heavy-hole band that are degenerate at their zone-center maxima. This configuration is labeled Ge(4;2). In unstressed Ge, it is well established that the EHL is stable with respect to excitons at low temperature.[1–8] The stability of the EHL

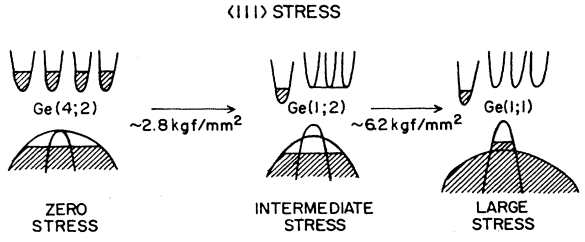

FIG. 1. The band structure of germanium as a function of ⟨111⟩ stress [after Ref. 1(b), Chap. 3, Fig. 6]. At zero stress all four conduction bands are occupied, as are both valence bands. At a stress of $\simeq 2.8$ kgf/mm^2, the three raised conduction bands are emptied, while both valence bands remain occupied. At stresses $\gtrsim 6.2$ kgf/mm^2, only one conduction band and one valence band are occupied.

is a consequence of the highly degenerate band structure. Different theoretical groups[2-8] have calculated values of the EHL ground-state energy, finding values that are 1.0–1.2 exciton rydbergs lower than the exciton ground state. Experimental results are in excellent agreement with the lower of these values. The corresponding ground-state density of 2.2×10^{17} cm^{-3} has also been confirmed experimentally by several researchers.[1]

The properties of the EHL change considerably when the crystal is stressed. At a $\langle 111 \rangle$ stress of about 2.8 kgf/mm^2 (1 kgf/mm$^2\equiv$10 MPa), the splitting between the raised and lowered conduction bands becomes greater than the electron Fermi energy, and only the lowered valley is occupied. This configuration is labeled Ge(1;2). At stresses greater than 6 kgf/mm^2, the hole-band splitting becomes larger than the hole Fermi energy, and only the upper hole band is occupied. This configuration is labeled Ge(1;1). At low stresses, the raised hole band is warped due to the proximity of the lowered band. However, at stresses above 70 kgf/mm^2, the occupied band is well described by an ellipsoidal dispersion relation.[9] Theoretical calculations of the system's properties in this "high-stress limit" are thus greatly simplified.

In stressed Ge, the considerable reduction in the band degeneracy causes a decrease in the binding energy of the EHL. There has been a long-standing question over whether the EHL is the stable phase in the limit of high $\langle 111 \rangle$ stress. In contrast to the unstressed case, different theoretical groups[2-8] have come to conflicting conclusions as to whether $E_G < -\phi_x$ in highly stressed Ge. These calculations use different approximations to model the many-body correlation energy $E_c(n)$. Experimental studies such as those reported here can test the validity of these approximation schemes.

Early calculations of the EHL ground-state energy for Ge(1;1) were done using the Pines-Nozières[4,10] interpolation scheme and the Hubbard approximation.[3,11] These methods predicted values of ϕ_l that were so small ($\lesssim 0.1\phi_x$) that the EHL stability could not be conclusively determined. Vashishta *et al.*[2,7,8] have undertaken an extensive series of calculations using the fully-self-consistent formulation of Singwi, Tosi, Land, and Sjölander (STLS).[12] They conclude that the EHL will definitely be bound in Ge(1;1). In contrast, Chakraborty and Pietiläinen[6] have applied a variational approach to the EHL ground state. They conclude that the EHL is not bound in Ge(1;1). They have commented that all the calculational schemes contain uncontrolled approximations, and that the uncertainty in these results may be too large to make a definitive conclusion.[13] It appears that the question will have to be decided experimentally.

Experimental studies[14-19] to date have reported density measurements up to stresses of 44 kgf/mm^2, which is below the high-stress limit. These authors have mostly used uniform-stress techniques. In practice, it is difficult to obtain these and higher stresses via uniaxial pressure without breaking the sample. However, experimental studies of the EHL in the high-stress limit in silicon[20] have been successful due to the use of the Hertzian strain-confinement geometry.

Theoretical predictions and experimental measurements of the electron-hole enhancement factor $g_{eh}(0)$ have also been reported.[2,3,6,16,21] This quantity is the electron-hole spatial correlation function evaluated at zero electron-hole separation and normalized to the average liquid density. Its measurement can provide a sensitive test of different approximations used in many-body calculations, since it is much more model dependent than other theoretically predicted quantities such as the density or the ground-state energy. Chou and Wong[16] have reported the first measurement of $g_{eh}(0)$ in Ge as a function of $\langle 111 \rangle$ stress up to 15 kgf/mm^2. Their analysis was based on assumptions about the density dependence of the EHL lifetime because no lifetime measurements were available. Culbertson and Furneaux[21] report an absolute measurement of $g_{eh}(0)$, but the uncertainties associated with their technique are quite large.

In this paper, we report experimental measurements of the density of the EHL in GE up to 87 kgf/mm^2, which is well into the high-stress limit, using strain-confinement techniques. Our results confirm previous measurements of EHL density at stresses $\lesssim$44 kgf/mm^2, and find a high-stress value of the EHL density at 2 K that is in good agreement with the results of calculations[5] based on the STLS method. In addition, our measurements of EHL density and lifetime have been combined to yield the surprising result that the enhancement factor $g_{eh}(0)$ appears to be constant for EHL densities $\gtrsim 3.5\times10^{16}$ cm^{-3}. This result is of significance because it contradicts theoretical predictions of the behavior of $g_{eh}(0)$ with density while remaining in agreement with previous experimental measurements.[21] Both of these experiments serve as important tests for the approximation schemes used in theoretical many-body physics.

II. EXPERIMENTAL APPARATUS

Ultrapure crystals of dislocation-free[22] Ge ($|N_A-N_D|<2\times10^{11}$ cm^{-3}) were used in these studies. The compressive force was applied by a pushrod and either a calibrated valve spring or hydraulic press mounted on top of a sample holder in an optical cryostat. The stressing apparatus is similar to that of Gourley and Wolfe.[20] The sample temperature was regulated with liquid or gaseous helium. Carriers were photoexcited by an acousto-optically modulated Nd:YAG (neodymium-doped yttrium aluminum garnet) laser with a wavelength of $\lambda=1.064$ μm. Recombination luminescence was collected by an 85-mm $f/1.5$ lens that focused a 5$\times$ magnified image of the sample onto the entrance plane of a $\frac{1}{2}$-m spectrometer. Between the collection lens and spectrometer, the image was reflected from two precision galvanometer motor-controlled mirrors, one rotating vertically and the other horizontally. The galvanometer controlled mirrors could scan the sample image across the entrance aperture with high accuracy for selective spatial sampling of the luminescence. The image of the sample could also be raster scanned in an X-Y pattern, with the luminescence intensity for each position in a 256$\times$256 array producing a spatial image of the sample luminescence, as discussed by Greenstein and Wolfe.[23]

The luminescence was detected by a cooled Ge photo-

diode or PbS photoconductive detector mounted at the exit slit of the spectrometer. The Ge photodiode was sensitive to recombination signals with $\lambda < 1.78$ μm, corresponding to ⟨111⟩ stresses of $\lesssim 25$ kgf/mm^2 in Ge. Its output was fed to a low-noise preamplifier followed by a lock-in amplifier to record spectra, or to a high-speed preamplifier followed by a transient recorder and digital-signal analyzer to record luminescence time decays. The PbS detector is sensitive to $\lambda = 1-4$ μm and was used to record spectra for ⟨111⟩ stresses greater than 25 kgf/mm^2. Its output was preamplified and fed into the lock-in amplifier for spectral data acquisition. Its slow time response ($\lesssim 100$ Hz) prevented its use in spatial and time-decay measurements.

III. STRAIN CALIBRATION

A first series of pure uniaxial ⟨111⟩-stress measurements were performed on a long, thin ($1.3 \times 1.6 \times 8.3$ mm^3) ⟨111⟩-oriented sample compressed on both ends by $\frac{1}{4}$-in.-diam ball bearings. The incident laser power was chosen to be low enough ($\simeq 76$ mW) so that sample heating was insignificant. By imaging the luminescence from the sample at the highest stress used ($\simeq 12$ kgf/mm^2), the electron-hole drops (EHD) were found to drift from the excitation spot to the opposite face due to the slight strain gradient still present. Therefore, by measuring the EHL peak position near the excitation spot and on the opposite side of the crystal, the magnitude of the residual strain gradient could be determined. It was found to be 0.5 meV/mm for this worst (highest-stress) case. Thus, as luminescence for the uniform-stress experiment was collected from a 100-μm spatial region in the middle of the crystal, there was a broadening of less than 0.05 meV in the EHL line shape due to the gradient. This value was less than the experimental resolution.

Plots of the free-exciton (FE) and EHL peak positions versus stress obtained in this experiment are shown in Fig. 2. The relative values of stress were determined using the measured spring constant and compression to obtain the force and then dividing by the cross-sectional area of the sample. The zero-stress energies were obtained from a completely unclamped sample. To account for the friction force present in the stressing mechanism, a constant 1.5 kgf/mm^2 was added to the nonzero stresses. This value was obtained by normalizing the data to high-resolution absorption measurements,[24] which show that the zero-stress intercept of a line drawn through the stressed exciton peak positions should be $\simeq 0.8$ meV above the unstressed exciton peak position. The slope of the line drawn through the exciton peak positions in Fig. 2 (0.79 meV mm^2/kgf) agrees well with that measured in Ref. 24 (0.78 meV mm^2/kgf) and essentially gives the rate of change of the band gap with stress.

The EHL peak position does not shift with stress for stresses below approximately 3 kgf/mm^2, due to a decrease in liquid binding energy with increasing stress. Above this stress, the stress-split upper conduction-band valleys are completely depopulated, and the EHL peak roughly follows the FE peak. The EHL luminescence also narrows significantly as stress is applied which is

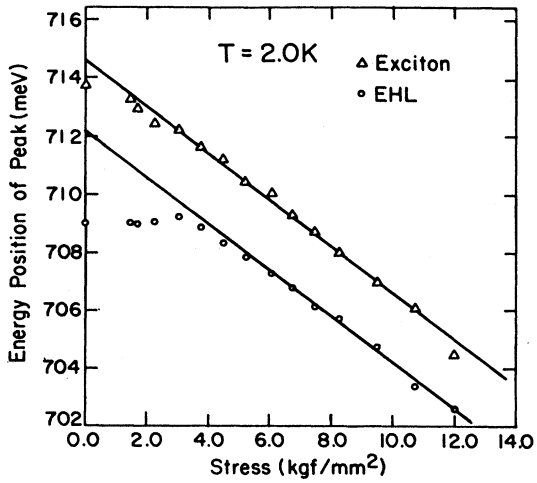

FIG. 2. FE and EHL peak positions in energy vs. uniform ⟨111⟩ stress. The EHL peak does not shift until the upper stress-split conduction-band valleys become depopulated ($\gtrsim 3$ kgf/mm^2).

consistent with a reduction in EHL density. The values of density and of hole and electron Fermi energies are derived from theoretical fits to the luminescence spectra and will be presented in a subsequent section.

Another way to study the properties of EHL in ⟨111⟩-stressed Ge is to take advantage of a strain-confinement technique developed by the Berkeley group.[25] When a crystal is stressed by a rounded plunger, the resulting shear strain distribution exhibits a maximum inside the crystal and not on the surface contact point. As the band gap decreases with increasing shear strain, the band gap has a minimum inside the crystal. The detailed stress distribution is quite complicated, but the important feature is that a small pocket of maximum uniaxial stress is created within the sample at a distance $z_m \propto (FR)^{1/3}$ below the sample surface,[20] where R is the plunger radius and F the applied force. The sample can be quite large in relation to the high-stress pocket, and large gradients in surface stresses that cause fractures can be avoided. The point of maximum stress is the point of maximum band-gap reduction. Thus, the high-stress pocket serves as a spatial potential well that attracts the carriers created at the surface.

Detailed analyses[20,26,27] have been done on the strain and band-gap distribution for Hertzian-stressed samples. Overall, the strain distribution is highly nonuniform. However, if the EHL is confined to a small enough region around a strain maximum (energy minimum), the strain is approximately uniform. Specifically, when the plunger is aligned along the ⟨111⟩ direction, the local region at the center of the well is nearly equivalent to a uniform uniaxial ⟨111⟩ stress.[27] (Obviously, the degree of uniformity is an important factor in our experiments.) It is this property of the Hertzian strain geometry that makes it suitable for our studies. In practice, a single large drop of EHL collects in the strain well with a radius dependent upon the generation rate G of electron-hole pairs and the

recombination lifetime τ. Specifically, the steady-state number of pairs is

$$N=\varepsilon G\tau \ , \tag{2}$$

with ε being the efficiency with which photoexcited pairs initially created at the crystal surface are collected in the strain well. In the absence of compression, the radius of the drop is simply

$$R=(3N/4\pi n_0)^{1/3} \ , \tag{3}$$

n_0 being the EHL density. A typical radius is $\simeq 100\ \mu$m for a few mW excitation power.

In the region of highest strain, the local variation in the semiconductor's band-gap subjects electron-hole pairs to a harmonic-oscillator potential of the form

$$E=E_0+\alpha r^2 \ , \tag{4}$$

where E_0 is the energy at the bottom of the well, r is the distance of the pair from the bottom of the well, and α is a constant that characterizes the curvature of the well.

There are two advantages in using the strain-well technique for the present experiment. First, in all "uniform-stress" geometries there are regions of the sample that are under much greater stress than the region of interest (e.g., where a corner of the crystal contacts the stressor), and this can lead to crystal fracture when very large stresses are applied. In the strain-well geometry, the maximum stress point is precisely the region of interest, and it is located inside the sample where the crystal is structurally strongest. The second advantage of the strain-confinement technique is that it enables the true EHL bulk lifetime to be measured as a function of stress. In uniform-stress experiments such as the one described above, recombination at the crystal surfaces and FE boiloff can shorten the observed lifetimes to values far below volume decay rates. The strain well, however, inhibits FE boiloff and confines the EHL to the inside of the crystal—enabling measurements of the true EHL volume decay rate to be performed.

Control over the curvature of the strain well [the parameter α in Eq. (4)] was a very important part of this experiment. The EHL in stressed Ge is highly compressible[28] and low values of α and low laser powers were necessary to avoid compression of the liquid which changes its density and distorts the luminescence spectra. Nylon stressors which were used in the first strain-well experiments[25] yielded values of α in the range of 5 to 10 meV/mm^2, but would plastically deform under the large stresses required in this experiment. Plungers cut from stainless-steel ball bearings can handle the large stresses, but create strain wells with much larger values of α. After some experimentation, it was found that a plunger cut from a 3-in.-diam ball bearing padded with a 20-mil sheet of Mylar R would yield acceptable values of α over the range of stresses used here (5–87 kgf/mm^2).

The method described by Gourley and Wolfe[29] was used to measure α experimentally in the Hertzian strain well. The strain well can be treated as a harmonic-oscillator potential for excitons. If the excitons are treated as a classical gas, it can be shown that the requirement of spatial invariance of the chemical potential[30] leads to the following expression for the spatial distribution of excitons:

$$n_{\rm ex}(r)=n_0 e^{-\alpha r^2/k_B T} \ , \tag{5}$$

where r is the radial distance from the center of the well, n_0 is the density of excitons at the center of the well, k_B is Boltzmann's constant, and T is the temperature. The full width at half maximum (FWHM) of this distribution is given by

$$(2.77k_B T/\alpha)^{1/2} \ . \tag{6}$$

Thus, one can obtain α from the spatial FWHM of the exciton distribution at a given temperature. Results of such measurements at several different stresses where the Ge photodiode was sensitive yielded values of α in the range of 5–8 meV/mm^2. The value of α is weakly dependent on stress.[20]

IV. LUMINESCENCE DATA

Luminescence spectra from the EHL LA-assisted phonon replica were recorded from uniformly stressed crystals for stresses from 1.0 to 12 kgf/mm^2, and from Hertzian-stressed crystals for stresses from 5.6 to 87 kgf/mm^2. Three representative spectral scans (solid lines) are shown in Fig. 3, corresponding to ⟨111⟩ stresses of 87, 44, and 0 kgf/mm^2 (unstressed). The dotted curves are theoretical fits to the data. The theoretical EHL spectral line shape is generated by the convolution of the occupied electron and hole densities of states:

$$I(\nu,h\nu')=I_0\int_0^\infty d\varepsilon\,|M|^2 D_e(\varepsilon)f(\varepsilon-E_F^e) \times D_h(h\nu'-\varepsilon)f(h\nu'-\varepsilon-E_F^h) \ , \tag{7}$$

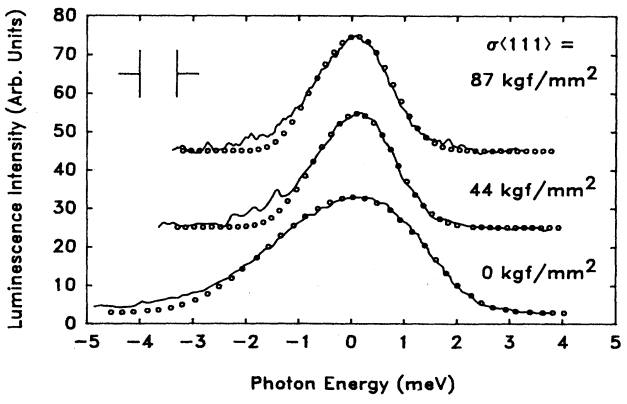

FIG. 3. Three EHL luminescence spectra at $T=2$ K for different values of the applied stress: 0, 44, and 87 kgf/mm^2. The spectra have been shifted in energy for clarity. The actual peak positions are 709, 677, and 643 meV, respectively. The dotted lines are theoretical fits, yielding EHL densities of 2.1×10^{17}, 1.1×10^{16}, and 9.8×10^{15} cm^{-3} for 0, 44, and 87 kgf/mm^2, respectively.

where $f(x)=(e^{\beta x}+1)^{-1}$ is the Fermi function, M is the matrix element, $\beta=(k_B T)^{-1}$, and D_e and D_h are the densities of states of the electrons and holes. The constant I_0 is a normalization factor. We use the stress- and energy-dependent densities of states calculated by Kelso.[9] Fits of the data to this line shape, taking into account the spectral resolution, yield values of the Fermi energy $E_F=E_F^e+E_F^h$, where E_F^e is the electron Fermi energy and E_F^h is the hole Fermi energy. The carrier density in the EHL is then given by

$$n_{e,h}=\int_0^\infty D_{e,h}(E)f(E-E_F^{e,h})dE \ . \tag{8}$$

The quantities E_F^e and E_F^h are not independent, because charge neutrality requires that $n_e=n_h$. When generated to match the full width at half maximum of the EHL spectra, the line shape (7) leaves some unfit luminescence on the low-energy side of the EHL spectral peak. This low-energy luminescence has been attributed to finite-lifetime effects[31,32] in the EHL as well as to pair recombination assisted by forbidden transitions.[33,34]

In our experiments, we sought to measure the equilibrium densities of the EHL as a function of stress. Since the EHD are highly mobile in strain gradients[35] and the EHL in Ge is highly compressible,[28] the spatial potential of the strain well can cause the liquid to be compressed to a density significantly higher than its equilibrium value. This compression effect is demonstrated in the data of Figs. 4(a)–4(d), in which the fit EHL density (discrete points) is plotted as a function of incident laser power for several representative stresses. The EHL densities for all the data points are obtained by fitting the spectra with a single, uniform-density EHL line. At all stresses, the density is seen to be higher for higher laser powers, due to the larger inward force of the well on the larger electron-hole droplets. The data taken at the two lower stresses ($\sigma=12$ and 23 kgf/mm^2) exhibits a plateau in EHL density for incident laser powers less than 200 μW (in the 12-kgf/mm^2 data) and 100 μW (in the 23-kgf/mm^2 data). In these cases, the plateau in EHL density at low powers indicates that the liquid density measured at these powers is the uncompressed equilibrium value.

The PbS detector was used at stresses above 25 kgf/mm^2. In this higher-stress regime, the density of the EHL in the strain well does not exhibit a clear plateau at the lowest laser powers [e.g., the data at stresses of 44 and 87 kgf/mm^2, Figs. 4(c) and 4(d)]. One can see from these data the principal difficulty in such experiments. To approach the equilibrium EHL density, detection of relatively high-resolution luminescence spectra for very small excitation powers, $\lesssim 10$ μW, is required. We see, however, that at 10 μW the EHL density in Figs. 4(c) and 4(d) have nearly reached the equilibrium values. For example, at 87 kgf/mm^2 an order-of-magnitude change in power produces only a 30% change in EHL density.

We can quantitatively describe the power dependence of all of these strain-well spectra from the following analysis. The EHL density as a function of the radius r from the center of a strain-confined electron-hole droplet of radius R is given by[23,36,37]

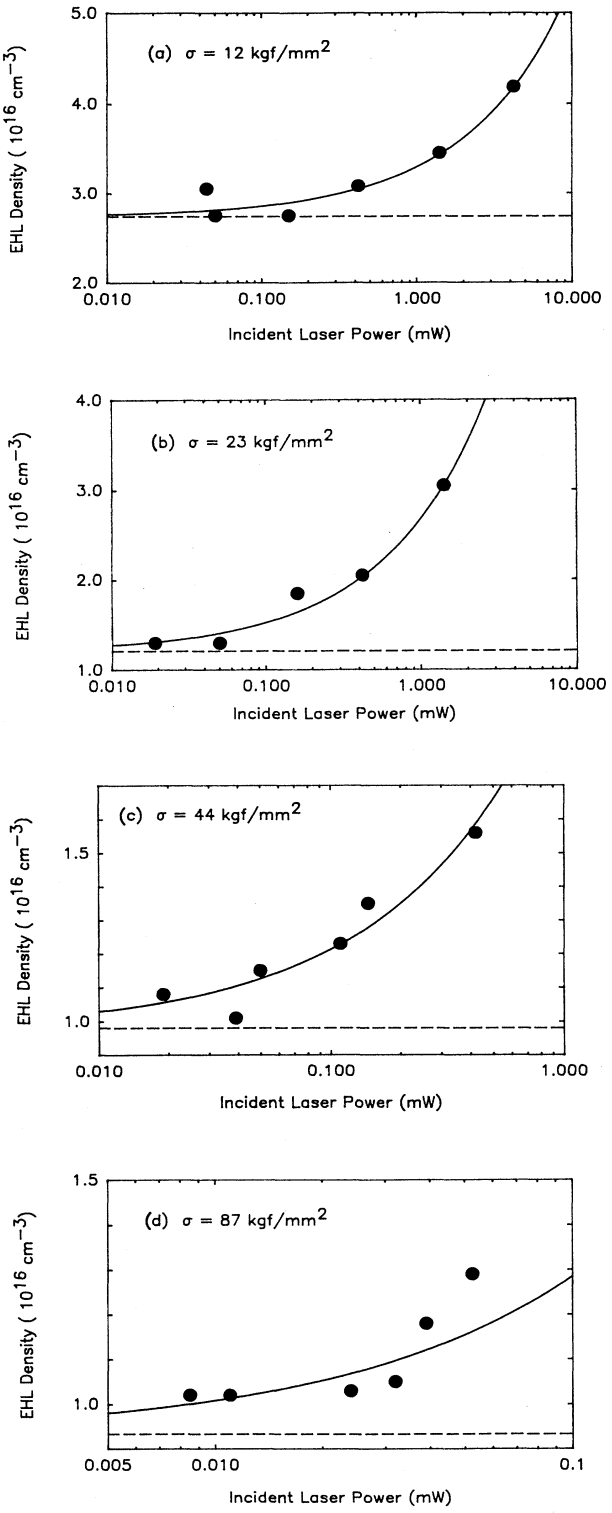

FIG. 4. Plot of the fitted density of strain-confined EHL vs incident laser power at $T=2$ K at several ⟨111⟩ stresses of (a) 12, (b) 23, (c) 44, and (d) 87 kgf/mm^2. The solid lines are fits to the relation $n=n_0+bP^{2/3}$ (see text). The dashed lines indicate the value of n_0 in the fitting function. Typical values of the well parameter α were $\simeq 10$ meV/mm^2 (measured at stresses below 23 kgf/mm^2).

$$n(r)=n_0\left[1+\frac{\alpha R^2}{n_0^2 E_0''}\left[1-\frac{r^2}{R^2}\right]\right], \tag{9}$$

where n_0 is the uncompressed EHL density at a given stress and temperature, and E_0'' is d^2E/dn^2 evaluated at $n_0(T)$, where E is the ground-state energy per pair of the liquid. The above expression is valid at low T, where the conditions $k_BT/E_F \ll 1$ and $k_BT/(E_F-E_{\rm spl}) \ll 1$ are satisfied for both electrons and holes, where $E_{\rm spl}$ is the splitting of degenerate bands due to stress. Numerical calculations by Schowalter *et al.*[38] of the composite spectrum expected for a strain-confined droplet of compressed EHL indicate that the spectrum is dominated by the mass of liquid that is near the center of the well and that is under the greatest compression. Thus, the single-density fits to our compressed spectra may be considered to represent the EHL density at the center of the strain well, which is given by

$$n_m=n(r=0)=n_0\left[1+\frac{\alpha R^2}{n_0^2 E_0''}\right]. \tag{10}$$

Some measurements of the droplet radius were possible with the Ge photodiode at stresses below $\sigma=24$ kgf/mm^2. At higher stresses, the slow time response of the PbS detector made spatial imaging of the strain-confined droplets at low laser powers impractical, thereby preventing measurements of the droplet radius R. In order to relate n_m to the incident power P, we approximate the droplet radius R by combining equations (2) and (3), viz.,

$$N=\varepsilon G\tau=4\pi R^3 n_0/3\ , \tag{11}$$

where the surface-generation rate G is linearly proportional to the laser power, $G=P/h\nu_{\rm laser}$. Substituting the above relation between R and P into Eq. (10), we obtain the following relation between n_m and P:

$$n_m=n_0+bP^{2/3}\ . \tag{12}$$

The parameters α, $h\nu$, n_0, E_0'', ε, and τ have all been absorbed into the parameter b.

Fits of the relation (12) to the density-versus-power plots in Fig. 4(a)–4(d) are shown as the solid lines. In each case, the fit value of n_0 is shown as the dotted line. The fit values of n_0, the uncompressed EHL density, allow us to estimate the amount of compression in the measured EHL densities. Values of the zero-compression extrapolations (indicated by dotted lines in Fig. 4) are typically within 10% of the densities obtained from the spectra taken at the lowest powers. The good agreement between the extrapolated and measured densities gives us confidence that our spectral measurements reflect the equilibrium densities of the EHL.

V. EHL DENSITY RESULTS

The values of the Fermi energies found from our lowest power spectral data are plotted versus ⟨111⟩ stress in Fig. 5(a) for electrons and Fig. 5(b) for holes. The resulting values of the EHL density are plotted versus stress in Fig. 6. The data show the behavior expected from the changes in the band structure. A large density decrease, more than threefold, occurs in going from the unstressed configuration to an applied stress of $\sigma\simeq 3$ kgf/mm^2. This decrease is due to the emptying of the raised electron valleys, with the concomitant reduction in the density of states. A more gradual decrease is observed at higher stresses, as the hole density of states approaches the infinite-stress form.

A long-open question in this field has been: is the EHL stable with respect to the formation of an excitonic gas in the limit of infinite ⟨111⟩ stress? Several calculations[2,5,7,8] using the STLS approximation technique have predicted the EHL to be stable in this regime. In contrast, other results[3,4,6] have predicted that the EHL is not bound, or are inconclusive. We have observed the EHL phase at $\sigma=87$ kgf/mm^2, which is in the high-stress lim-

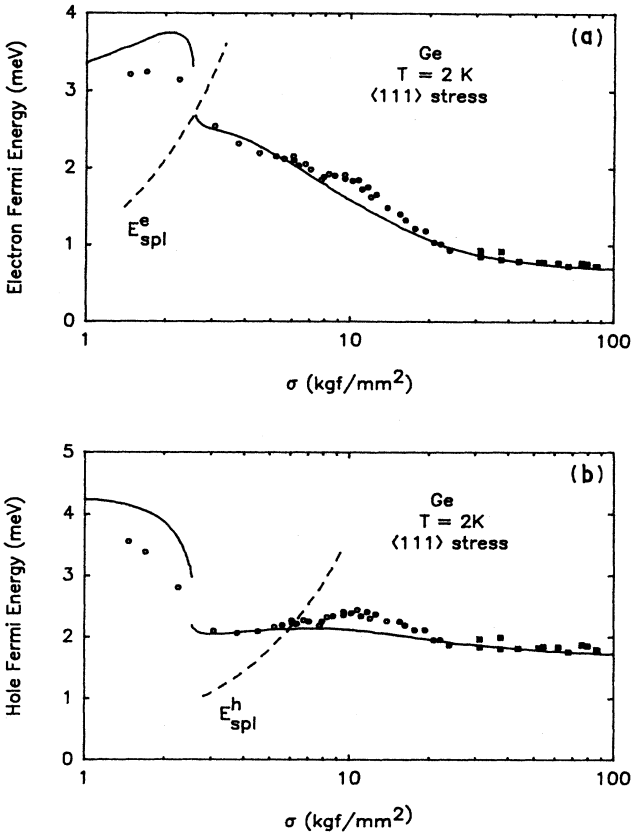

FIG. 5. Plot of the fitted Fermi energies of (a) electrons and (b) holes as a function of applied ⟨111⟩ stress at $T=2$ K. The uniform-stress data are represented with open circles. Solid circles correspond to Ge-detector data. The data recorded at high stresses with the PbS detector are represented with solid squares. The dashed lines denote the splittings within the electron and hole bands. The solid curves are theoretical results (Ref. 5, model 1) for $T=2$ K. The crossing of the dashed and solid lines give the stresses at which the stress-split bands are emptied.

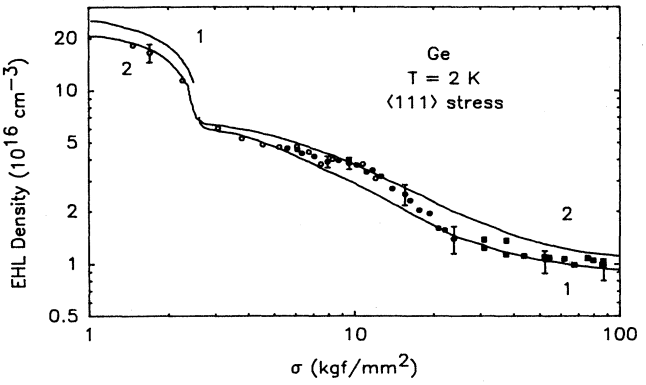

FIG. 6. EHL densities at $T=2$ K as a function of uniaxial ⟨111⟩ stress. The uniform-stress data are represented with open circles. Solid circles correspond to Ge-detector data. The data recorded at higher stresses with the PbS detector are represented with solid squares. The solid curves are theoretical calculations (Ref. 5, models 1 and 2) for the stress-dependent EHL density at $T=2$ K.

it. This result is a strong confirmation of the accuracy of the STLS approximation[2,5,7,8] in predicting the ground-state parameters of this system.

Kelso[5] has done a systematic theoretical study of EHL properties using several models. The results of her $T=2$ K calculations are shown as the solid lines in Figs. 5 and 6. Curve 1 in Fig. 6 was generated using an exchange-correlation energy of the STLS form,[8] while curve 2 was based on an exchange-correlation energy of the Wigner form.[39] Both are in good agreement with our results for the Fermi energies and EHL density.

The present results are also in good agreement with previous measurements[14–18] for stresses below $\simeq 35$ kgf/mm^2. For the stress range 35–45 kgf/mm^2, our lowest directly observed densities are $\simeq 10$–20% larger than the uniform-stress results of Kukushkin and Kulakovskii,[19] but our zero-compression extrapolations are in close agreement with their data. Taking into account compression effects and the change in the hole mass, we estimate the EHL density to be $(9\pm2)\times10^{15}$ cm^{-3} at $T=2$ K in the limit of infinite stress.

VI. EHL LIFETIME RESULTS

Lifetimes for decay of the EHL luminescence were recorded in the strain-confinement geometry in the lower-stress range where the Ge photodiode was sensitive ($\sigma \lesssim 24$ kgf/mm^2). The inverse lifetime values are plotted versus EHL density in Fig. 7(a). Note that most of the range of EHL densities measured in these experiments is covered by the data presented Fig. 7(a). At the highest stress for which the Ge photodiode is sensitive ($\sigma=23.9$ kgf/mm^2), the EHL density is only 40% larger than that measured at 87 kgf/mm^2 with the PbS detector.

The lifetime measurements provide another means of testing different many-body approximation schemes used in the calculation of EHL ground-state parameters. In particular, the EHL lifetime is sensitive to the value of the electron-hole enhancement factor $g_{eh}(0)$, which is defined as the increase in probability of finding an electron at the position of a hole compared to the corresponding probability for uncorrelated carriers. The enhancement factor has been predicted to increase as the EHL density decreases, but the rate at which it does so is dependent upon the theoretical model used.[26]

The total decay rate for EHL in Ge can be expressed[36] as

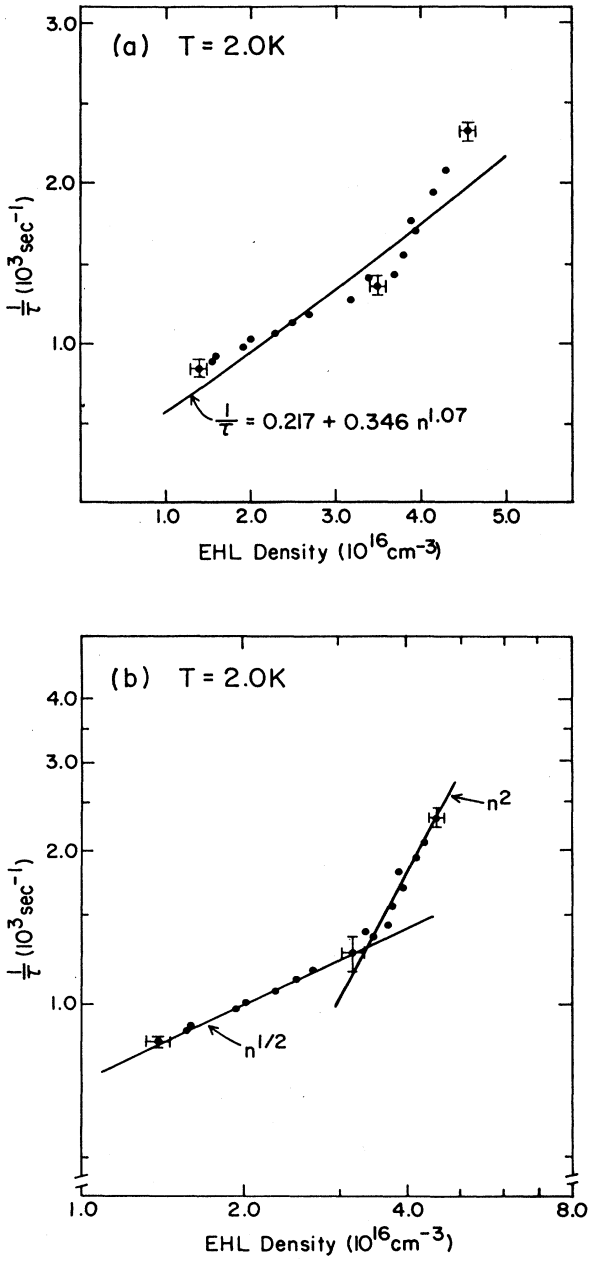

FIG. 7. Inverse EHL lifetime vs density on (a) linear and (b) double-logarithmic scales. The solid line in (a) is a least-squares fit to the data using Eq. (14) with $B=0$.

$$\tau^{-1} = A + Bg_{eh}(0)n + C[g_{eh}(0)n]^2 = \tau_i^{-1} + \tau_r^{-1} + \tau_a^{-1} , \quad (13)$$

where τ_i^{-1} is a density-independent term due to decay at impurities, τ_r^{-1} is the radiative decay rate, and τ_a^{-1} is the decay rate due to a phonon-assisted Auger decay process [Ref. 1(a)]. Because there are so many terms in the equation for the decay rate (all of which can be important) it is difficult to determine the actual density dependence of $g_{eh}(0)$ from the τ^{-1} versus n data. However, the theoretical results can be checked for consistency with the data shown in Fig. 7(a). In particular, the fully-self-consistent (FSC) calculation of Vashishta *et al.*[2] predicts that $g_{eh}(0) \propto n^{-0.465}$ for the range of EHL densities obtained in the present experiment. If this expression is substituted into Eq. (11), the EHL decay rate becomes

$$\tau^{-1} = A + Bn^{0.535} + Cn^{1.07} . \quad (14)$$

Using this equation, the most rapid density dependence possible for τ^{-1} would occur if $B=0$, and a least-squares fit to the data for this case is shown in Fig. 7(a). Clearly, this still underestimates the true density dependence of the decay rate. It is possible that a term of order $[g_{eh}(0)n]^3$ could be included in the description of the EHL decay rate; however, this would correspond to a four-particle recombination process, which is expected to be orders of magnitude less important than those considered above [Ref. 1(a)].

Shrivastava has published first-principles calculations[40] that indicate that terms of order $[g_{eh}(0)n]^{5/3}$ and $[g_{eh}(0)n]^{4/3}$ should also be included in a description of the Auger decay rate. These are obtained by including the wave-vector dependence of both the interband Coulomb interaction and the electron-phonon interaction in the calculation of the Auger rate. But, they would still not increase the overall density dependence of Eq. (13).

The inverse-lifetime–versus–density data are plotted on a double-logarithmic scale in Fig. 7(b). It shows that a term in the expression for the decay rate of order n^2 is necessary to describe the data for EHL densities greater than 3.5×10^{16} cm^3. This would imply that $g_{eh}(0)$ is virtually independent of density—a surprising result. However, if one uses the recent theoretical results for the phonon-assisted Auger decay rate[40] to model the density dependence of the EHL decay rate in Si (see Ref. 20), one also obtains that $g_{eh}(0)$ is independent of density. In fact, this is also consistent with the results of recent experimental measurements of $g_{eh}(0)$ by Culbertson and Furneaux.[21] Their results are in quantitative agreement with the FSC calculation, but the experimental uncertainties were large enough that a density-independent $g_{eh}(0)$ could also fit their data. Clearly, more theoretical work on the density dependence of the electron-hole correlation factor is warranted.

VII. CONCLUSIONS

These experiments are the only ones that have examined the excitonic system in Ge in the limit of high ⟨111⟩ stress. They have also revealed an interesting disagreement between theory and experiment concerning the electron-hole enhancement factor $g_{eh}(0)$. Our success in obtaining these results is of experimental and theoretical importance. Experimentally, we have demonstrated the very clear advantage that the Hertzian well offers in probing the properties of the EHL in stressed semiconductors. Theoretically, our results are a demonstration of the success of many-body calculations in predicting the ground-state energy and density of the EHL, but also show the greater difficulty they have in predicting its microscopic structure. Studies of this system can provide useful information using these tools.

ACKNOWLEDGMENTS

This work was supported by the National Science Foundation under Grants No. DMR-80-20250 and No. DMR-80-24000, with facility support from the Materials Research Laboratory. A. H. Simon was supported in part by the Shell Foundation. The high-purity Ge samples were provided by E. E. Haller.

*Present address: East Fishkill Facility 300-48A, IBM Corporation, Route 52, Hopewell Junction, NY 12533-0999.

†Present address: Optoelectronics Division, Hewlett-Packard Company, Building 91-ML, 370 West Trimble Road, San Jose, CA 95131.

‡Address until August 1989: Physik-Department (E10), Technische Universität München, D-8046 Garching bei München, Federal Republic of Germany.

[1]Two volumes of general review articles on electron-hole droplets have appeared in the literature: (a) J. C. Hensel, T. G. Phillips, G. A. Thomas, and T. M. Rice, in *Solid State Physics,* edited by H. Ehrenreich, F. Seitz, and D. Turnbull (Academic, New York, 1977), Vol. 32; (b) *Electron-hole Droplets in Semiconductors in Modern Problems in Condensed Matter Series,* edited by C. D. Jeffries and L. V. Keldysh (North-Holland, Amsterdam, 1983), Vol. 6. For a review dealing specifically with the EHL in stressed Ge and Si, see G. K. Wong, in *Novel Materials and Techniques in Condensed Matter,* edited by G. W. Crabtree and P. Vashista (Elsevier Science, New York, 1982), p. 227.

[2]P. Vashista, S. G. Das, and K. S. Singwi, Phys. Rev. Lett. **33**, 911 (1974); P. Vashishta, P. Bhattacharya, and K. S. Singwi, Phys. Rev. B **10**, 5108 (1974).

[3]W. F. Brinkman, T. M. Rice, P. W. Anderson, and S.-T. Chui, Phys. Rev. Lett. **28**, 961 (1972).

[4]M. Combescot and P. Nozières, J. Phys. C **5**, 2369 (1972).

[5]S. M. Kelso, Phys. Rev. B **25**, 7631 (1982).

[6]T. Chakraborty and P. Pietiläinen, Phys. Rev. Lett. **49**, 1034 (1982).

[7]G. Kirczenow and K. S. Singwi, Phys. Rev. B **19**, 2117 (1979).

[8]G. Vignale, K. S. Singwi, R. K. Kalia, and P. Vashista, J. Phys. C **16**, 699 (1983).

[9]S. M. Kelso, Phys. Rev. B **25**, 1116 (1982).

[10]P. Nozières and D. Pines, Phys. Rev. **111**, 442 (1958).

[11]J. Hubbard, Proc. R. Soc. London, Ser. A **243**, 336 (1957).

[12]K. S. Singwi, M. P. Tosi, R. H. Land, and A. Sjölander, Phys.

Rev. **176**, 589 (1968).
[13]P. Vashishta, R. K. Kalia, and K. S. Singwi, Phys. Rev. Lett. **50**, 2036 (1983); T. Chakraborty and P. Pietiläinen, *ibid.* **50**, 2037 (1983). See also Lauri J. Lantto, Phys. Rev. B **36**, 5160 (1987).
[14]A. S. Alekseev, V. S. Bagaev, and T. I. Galkina, Zh. Eksp. Teor. Fiz. **63**, 1020 (1972) [Sov. Phys.—JETP **36**, 536 (1972)].
[15]C. Benoit à la Guillaume, M. Voos, and F. Salvan, Phys. Rev. B **5**, 3079 (1972).
[16]H.-h. Chou and George K. Wong, Phys. Rev. Lett. **41**, 1677 (1978).
[17]G. A. Thomas and Ya. E. Pokrovskii, Phys. Rev. B **18**, 864 (1978).
[18]B. J. Feldman, H.-h. Chou, and G. K. Wong, Solid State Commun. **24**, 521 (1977).
[19]I. V. Kukushkin, Zh. Eksp. Teor. Fiz. **84**, 1840 (1983) [Sov. Phys.—JETP **57**, 1072 (1983)].
[20]P. L. Gourley and J. P. Wolfe, Phys. Rev. B **24**, 5970 (1981).
[21]J. C. Culbertson and J. E. Furneaux, Phys. Rev. Lett. **49**, 1528 (1982); J. C. Culbertson, Ph.D. dissertation, University of California at Berkeley, 1982 (unpublished).
[22]The samples had a net active impurity concentration $|N_A - N_D| \simeq 2 \times 10^{11}$ cm^{-3}, and were grown by E. E. Haller and W. L. Hanson of Lawrence Berkeley Laboratory.
[23]M. Greenstein and J. P. Wolfe, Phys. Rev. B **24**, 3318 (1981).
[24]I. Balslev, Phys. Rev. **143**, 636 (1966).
[25]J. P. Wolfe, R. S. Markiewicz, S. M. Kelso, J. E. Furneaux, and C. D. Jeffries, Phys. Rev. B **18**, 1479 (1978).
[26]P. L. Gourley, Ph.D. dissertation, University of Illinois at Urbana-Champaign, 1980 (unpublished).
[27]R. S. Markiewicz, J. P. Wolfe, and C. D. Jeffries, Phys. Rev. B **15**, 1988 (1977).
[28]S. M. Kelso, Phys. Rev. B **26**, 591 (1982).
[29]P. L. Gourley and J. P. Wolfe, Phys. Rev. Lett. **40**, 526 (1978).
[30]L. D. Landau and E. M. Lifshitz, *Statistical Physics,* translated by J. B. Sykes and M. J. Kearsley, 2nd revised ed. (Pergamon, Oxford, 1969), p. 70.
[31]G. A. Thomas, E. I. Blount, and M. Capizzi, Phys. Rev. B **19**, 702 (1979).
[32]G. A. Thomas and M. Capizzi, in *Proceedings of the 13th International Conference on the Physics of Semiconductors, Rome, 1976,* edited by F. G. Fumi (North-Holland, Amsterdam, 1976), p. 914.
[33]R. W. Martin, Solid State Commun. **19**, 373 (1976).
[34]R. W. Martin and H. L. Stormer, Solid State Commun. **22**, 523 (1977).
[35]M. A. Tamor, M. Greenstein, and J. P. Wolfe, Phys. Rev. B **27**, 7353 (1983).
[36]S. M. Kelso and J. E. Furneaux, Solid State Electron. **21**, 1377 (1978); S. M. Kelso, Ph.D. dissertation, University of California at Berkeley, 1979 (unpublished).
[37]R. S. Markiewicz and S. M. Kelso, Solid State Commun. **25**, 275 (1978).
[38]L. J. Schowalter, F. M. Steranka, M. B. Salamon, and J. P. Wolfe, Phys. Rev. B **29**, 2970 (1984).
[39]H. Buttner, in *Festkörperprobleme XIII,* edited by H. J. Queisser (Pergamon, Vieweg, 1973), p. 145; E. P. Wigner Trans. Faraday Soc. **34**, 678 (1938).
[40]N. Shrivastava, Solid State Commun. **50**, 611 (1984).